Infection and Immunity

Mycobacterium marinum Infection of Adult Zebrafish Causes Caseating Granulomatous Tuberculosis and Is Moderated by Adaptive Immunity

Laura E. Swaim, Lynn E. Connolly, Hannah E. Volkman, Olivier Humbert, Donald E. Born and Lalita Ramakrishnan
***Infect. Immun.* 2006, 74(11):6108. DOI: 10.1128/IAI.00887-06.**

INFECTION AND IMMUNITY, Nov. 2006, p. 6108–6117 Vol. 74, No. 11
0019-9567/06/$08.00+0 doi:10.1128/IAI.00887-06

Mycobacterium marinum Infection of Adult Zebrafish Causes Caseating Granulomatous Tuberculosis and Is Moderated by Adaptive Immunity†

Laura E. Swaim,[1]‡ Lynn E. Connolly,[2]‡* Hannah E. Volkman,[3] Olivier Humbert,[1]§ Donald E. Born,[4] and Lalita Ramakrishnan[1,2,5]

Departments of Microbiology,[1] Medicine,[2] Immunology,[5] and Pathology[4] and Molecular and Cellular Biology Graduate Program,[3] University of Washington, Seattle, Washington 98195

Received 5 June 2006/Returned for modification 6 July 2006/Accepted 31 July 2006

The zebrafish, a genetically tractable model vertebrate, is naturally susceptible to tuberculosis caused by *Mycobacterium marinum*, a close genetic relative of the causative agent of human tuberculosis, *Mycobacterium tuberculosis*. We previously developed a zebrafish embryo-*M. marinum* infection model to study host-pathogen interactions in the context of innate immunity. Here, we have constructed a flowthrough fish facility for the large-scale longitudinal study of *M. marinum*-induced tuberculosis in adult zebrafish where both innate and adaptive immunity are operant. We find that zebrafish are exquisitely susceptible to *M. marinum* strain M. Intraperitoneal injection of five organisms produces persistent granulomatous tuberculosis, while the injection of ~9,000 organisms leads to acute, fulminant disease. Bacterial burden, extent of disease, pathology, and host mortality progress in a time- and dose-dependent fashion. Zebrafish tuberculous granulomas undergo caseous necrosis, similar to human tuberculous granulomas. In contrast to mammalian tuberculous granulomas, zebrafish lesions contain few lymphocytes, calling into question the role of adaptive immunity in fish tuberculosis. However, like *rag1* mutant mice infected with *M. tuberculosis*, we find that *rag1* mutant zebrafish are hypersusceptible to *M. marinum* infection, demonstrating that the control of fish tuberculosis is dependent on adaptive immunity. We confirm the previous finding that *M. marinum* ΔRD1 mutants are attenuated in adult zebrafish and extend this finding to show that ΔRD1 predominantly produces nonnecrotizing, loose macrophage aggregates. This observation suggests that the macrophage aggregation defect associated with ΔRD1 attenuation in zebrafish embryos is ongoing during adult infection.

Human tuberculosis, caused by *Mycobacterium tuberculosis*, results in a variety of outcomes that range from long-term asymptomatic infection to active disease (9, 14). The hallmark lesion of tuberculosis is the granuloma, an organized collection of differentiated macrophages: large epithelioid cells with tightly interdigitated cell membranes linking adjacent cells together (1). In addition, human tuberculous granulomas often contain lymphocytes and extracellular matrix and can undergo central necrosis that correlates with the gross appearance of caseous necrosis (1, 14). Necrotizing granulomas containing organisms are seen in active human tuberculosis (14, 15, 53). Chronic asymptomatic tuberculous infection of humans is characterized by fibrotic and calcified granulomas that may or may not contain viable bacteria (35). Necrosis likely plays an important role in tuberculosis morbidity and transmission, but the host and bacterial determinants required for its formation remain poorly understood (14).

Several animal models are used to study the pathogenesis and immunology of *M. tuberculosis* infection, each of which has its advantages and drawbacks (20). The commonly used mouse model produces poorly organized macrophage aggregates that do not undergo necrosis but has the advantage of abundant immunological and genetic tools and techniques (20). Guinea pigs and rabbits produce necrotizing granulomas (2, 15, 16, 29), but very few immunological and molecular reagents are available for these animals, which are also more expensive to maintain. Nonhuman primates appear to most faithfully mimic human tuberculosis (8), but their use is constrained by ethical and cost issues. These differences notwithstanding, cell-mediated adaptive immunity plays a critical role in the control of human tuberculosis and in all experimental mammalian models of tuberculosis where this has been assessed (21, 34).

The relatively rapidly growing human and animal pathogen *Mycobacterium marinum*, a close genetic relative of *M. tuberculosis* (49), is used to study the pathogenesis of tuberculosis (11, 14, 39, 46, 55). *M. marinum* causes systemic granulomatous infections and disease in its natural hosts, ectotherms such as fish and frogs, and peripheral chronic granulomatous disease (fish tank granulomas) in humans (10, 11, 19). Inoculation of the leopard frog produces a long-term, asymptomatic infection with well-defined, nonnecrotizing granulomas that harbor bacteria (5, 41). In contrast, experimental inoculation of goldfish, zebrafish, striped bass, or medaka produces necrotizing granulomas and ultimately lethal disease (7, 11, 12, 24, 39, 40, 48, 53, 54, 59).

The zebrafish is a commonly used laboratory animal for the study of development and disease (4, 50). Zebrafish are genetically tractable hosts: transgenic animals and random and targeted mutants can be created (14, 27, 31, 36, 58), its genome sequence is nearing completion (43), and microarray analysis using mRNA extracted from whole fish can be readily carried

* Corresponding author. Mailing address: Box 357242, University of Washington, Seattle, WA 98195. Phone: (206) 221-6367. Fax: (206) 616-1575. E-mail: lconnoll@u.washington.edu.

† Supplemental material for this article may be found at http://iai.asm.org/.

‡ L.E.S. and L.E.C. contributed equally to this work.

§ Present address: Molecular and Cellular Biology Graduate Program, University of Washington, Seattle, WA 98195.

out (30). Chemical and drug screens are also easily performed using this organism (37, 38). Zebrafish become infected with *M. marinum* in fish facilities (57) and also develop disease upon experimental inoculation (11, 12, 22, 23, 40, 54). A zebrafish embryo model of infection has been used to characterize the earliest events following mycobacterial infection in which macrophage aggregates with key features of tuberculous granulomas form (18). Because adaptive immunity is not yet operant at this early stage of development, the interactions of innate immunity with mycobacteria and their virulence determinants can be dissected in isolation (13, 52, 56).

Here, we describe a large-scale longitudinal analysis of *M. marinum* infection of adult zebrafish using the sequenced human strain M (42). Similar to a previous study using a fish-derived strain (40), we find a dose- and time-dependent mortality that is accompanied by increased bacterial burden and progressive granulomatous disease. In this study, we used inocula that are 2 to 5 logs lower than those reported previously by other groups (7, 22, 23, 40, 54) to demonstrate the exquisite sensitivity of the zebrafish to infection by *M. marinum* strain M. Although zebrafish possess adaptive immunity similar to that of mammals (50, 52), its role in controlling tuberculosis has not previously been determined. By infecting mutant zebrafish deficient in *rag1* (58), a recombinase required for the development of functional T and B cells, we demonstrate that adaptive immunity plays a critical role in controlling zebrafish tuberculosis as it does in mammalian tuberculosis (44). Finally, we find that an attenuated bacterial strain lacking the RD1 locus, which encodes a novel bacterial secretion system and displays a macrophage aggregation defect in zebrafish embryos (56), exhibits a similar defect in adult animals. This finding suggests that the RD1 locus plays similar roles throughout infection both in the context of innate immunity alone and in the presence of an adaptive immune response.

MATERIALS AND METHODS

Bacterial strains and growth conditions. *Mycobacterium marinum* strains used for this study were derived from a human clinical isolate, strain M (ATCC BAA-535), and were grown at 33°C in Middlebrook 7H9 broth (Difco) supplemented with 0.5% bovine serum albumin, 0.005% oleic acid, 0.2% glucose, 0.2% glycerol, 0.085% sodium chloride, and 0.05% Tween 80 or on Middlebrook 7H10 agar (Difco) supplemented with 0.5% bovine serum albumin, 0.005% oleic acid, 0.2% glucose, 0.2% glycerol, and 0.085% sodium chloride. Infected fish homogenates were plated onto 7H10 agar supplemented with amphotericin B (10 mg/liter), polymyxin B (20 mg/liter), trimethoprim (20 mg/liter), and carbenicillin (50 mg/liter) to avoid contamination with normal flora. Cultures used in infections were grown to an optical density at 600 nm of 1.0 and maintained at −80°C in 1-ml aliquots with 10% glycerol. CC1, a wild-type (WT) strain (12), and ΔRD1 (56), an attenuated strain, have been described previously.

Fish husbandry and genotyping. Zebrafish husbandry has been detailed previously by Cosma et al. (11). Briefly, the fish were reared in recirculating fish systems obtained from Aquatic Habitats (Apopka, FL) and transferred to a flowthrough fish system for the infection experiment. The flowthrough system prevents reinfection by allowing water to pass continuously through the tanks. Up to 12 fish were kept in each 9-liter tank, and tanks were maintained under conditions compliant with laboratory standards outlined by the Institutional Animal Care and Use Committee (water temperature of ~28°C, pH of ~7.4, and conductivity of ~1,500 μS).

Wild-type (family AB) founder zebrafish were originally obtained from David Raible's fish facility at the University of Washington. Heterozygous *rag1* mutant zebrafish (family Tübingen) obtained from Artemis Pharmaceuticals (Köln, Germany) (58) were spawned to produce isogenic siblings that were predicted to be approximately one-quarter mutant:one-half heterozygous:one-quarter wild type for *rag1*. Their genotype was determined at 3 to 6 months of age using DNA obtained from a tail clip procedure (57). Briefly, a small piece of fin was clipped from the fish and incubated in lysis buffer (100 mM Tris-HCl, 200 mM NaCl, 0.2% sodium dodecyl sulfate, 5 mM EDTA, 100 μg/ml proteinase K) overnight at 55°C. DNA was precipitated from the supernatant with isopropanol and then resuspended in water. To screen for the point mutation R797 that gives rise to a truncated Rag1 protein (58), the DNA was amplified by PCR with primers seq2F (5′-CCCTGACAGCCATCTTGGGAC-3′) and seq2R (5′-CGTGTCATCAGC CGACGAGC-3′). The 600-bp PCR product obtained was sequenced using the seq2F primer. The resulting sequence chromatograms were analyzed for the expected single nucleotide polymorphism (thymine-to-cytosine replacement) at one or both alleles.

Zebrafish infections and bacterial quantification. After lightly anesthetizing fish with 0.1% 3-aminobenzoic acid ethyl ester (tricaine), they were infected by intraperitoneal injection with 50 μl of thawed bacterial stocks that were diluted in phosphate-buffered saline (PBS) to obtain the desired inoculum. Bacterial CFU contained in the injected inoculum were confirmed at the time of infection by plating onto 7H10 agar. To assess the bacterial burden from whole fish at various time points postinfection, the fish were first bathed in 1.5 mg/ml kanamycin sulfate for 45 min at 27°C to inhibit contamination with normal flora. Following terminal anesthesia in 0.5% tricaine, fish were weighed and homogenized (model TH-115; Omni International, Marietta, GA) in 1.5 ml PBS in sterile polystyrene tubes. The homogenates were brought to a volume of 2.5 ml with PBS, and 10-fold serial dilutions were plated. Four to eight fish were plated for each condition per time point, and the resulting bacterial counts or CFU were determined.

Histology and microscopy. After terminal anesthesia, fish were fixed in Dietrich's fixative (57) for 72 h, transferred into 70% ethanol, and then sent to Histo-Tec Laboratories (Hayward, CA) for paraffin embedding, sectioning, and staining. Serial sagittal sections were used for hematoxylin and eosin and modified Ziehl-Neelson staining in all cases and additionally for Masson's modified trichrome (collagen) and Van Kossa (calcium) staining in some cases. Two to five fish from each infection dose at each time point were examined. Sections were examined under a Nikon E600 microscope (Tokyo, Japan), and images were collected with a digital photo camera (model DKC-5000; Sony, Tokyo, Japan) and produced using Metamorph software (Molecular Devices Corporation, Sunnyvale, CA). Final images were transferred to Adobe (San Jose, CA) Photoshop 7.0 to adjust levels and brightness (12, 56).

For a quantitative comparison of ΔRD1 and wild-type lesions, a blinded reviewer scored 121 granulomas from four wild-type-infected fish at 16 weeks and 126 granulomas from three ΔRD1-infected fish at 16 weeks in all tissues (kidney, liver, mesentery, pancreas, gonads, spleen, and head). All granulomas were assessed for the presence of necrosis and residence in a multicentric lesion. Nonnecrotizing lesions were further analyzed to assess the compactness of the macrophage association. The data were analyzed using contingency tables, assigning ΔRD1-infected fish as the experimental group and wild-type-infected fish as the control group, to determine the relative risk (RR) and 95% confidence intervals (CI). Significance was determined by Fisher's exact test.

Statistical analysis. Statistics were calculated using GraphPad Instat version 3.05 and Stata version 9.0. For the analysis of the bacterial growth curves, the data were found to not be normally distributed despite log transformation, so nonparametric tests (Mann-Whitney test for comparisons of two groups and Kruskal-Wallis test for comparisons between three or more groups) were used to determine significance. Medians were calculated using all fish, including those with bacterial burdens below the limit of detection.

RESULTS

***M. marinum* causes chronic, progressive disease of zebrafish in a dose-dependent fashion.** Adult zebrafish were injected with three doses of *M. marinum* or with PBS (mock), and survival and disease progression were assessed in two different cohorts of injected fish. Similar to previously published findings (40), a dose-dependent mortality was noted over the 16-week monitoring period (Fig. 1A). Most of the fish infected with 8,970 bacteria died within 2 weeks, whereas only 44% of the fish infected with 5 CFU of *M. marinum* died within the 16-week monitoring period. The fish infected with 60 CFU exhibited an intermediate mortality, with 83% being dead by 16 weeks. Only 11% of the mock-injected fish died during the 16-week period. Death of infected fish was preceded by re-

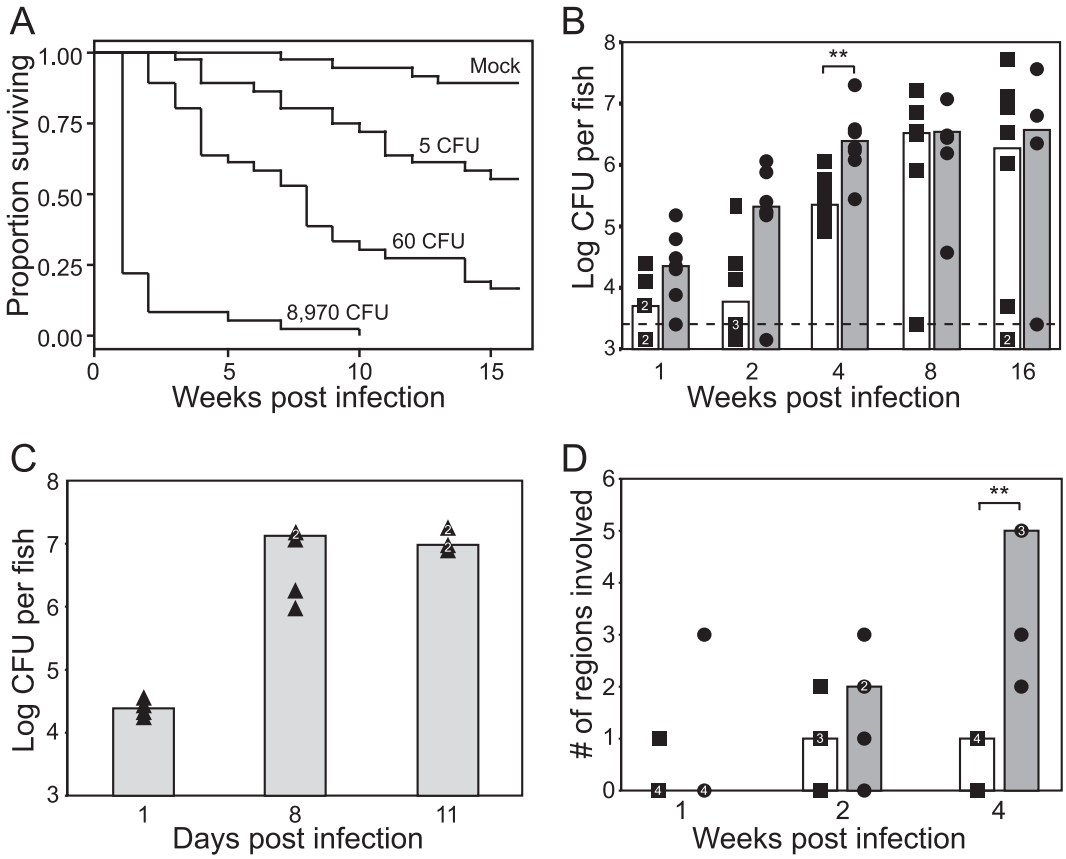

FIG. 1. Host death correlates with bacterial burden and disease dissemination. (A) Dose-dependent survival of adult zebrafish infected with wild-type *M. marinum*. Three separate tanks, each containing 12 fish at the indicated doses, were monitored for mortalities over a 16-week time period. No significant tank effects were detected, and the data from the three tanks were pooled for further analysis. A Kaplan-Meier curve was calculated for each dose as well as for mock-injected animals. Compared to mock-injected animals, each dose showed a significant difference in survival as calculated by log-rank test ($P < 0.001$). The Cox proportional hazards model was used to quantify group differences compared to mock-injected fish and confirmed significant differences in survival at each dose with the following hazard ratios (HR), 95% confidence intervals (CI), and *P* values: for the 5-CFU group, the HR was 4.85, the 95% CI was 1.6 to 14.5, and the *P* value was <0.005; for the 60-CFU group, the HR was 14.27, the 95% CI was 5.0 to 40.8, and the *P* value was <0.0001; for the 8.6×10^3-CFU group, the HR was 86.49, the 95% CI was 28.6 to 261.5, and the *P* value was <0.0001. (B and C) Dose-dependent growth of *M. marinum* in adult zebrafish. Fish in B were inoculated with 5 CFU (■) or 60 CFU (●) of WT *M. marinum*, while fish in C were inoculated with 8,970 CFU (▲), and bacterial counts were enumerated at the indicated time points. The limit of detection in these experiments (3.4 log CFU per fish) is indicated by the dashed line, and the number of fish falling below this limit at each time point is designated by a symbol underneath this line. Multiple fish at a given time point having the same bacterial counts are shown as a white numeral within the symbols (■, ●, or ▲). Median CFU are shown as overlying bar graphs (white for the 5-CFU group, dark gray for the 60-CFU group, and light gray for 8,970-CFU group). Significant differences in median bacterial loads at each time point were determined using the Mann-Whitney test (**, $P < 0.05$). (D) Fish infected with either 5 CFU (■) or 60 CFU (●) of *M. marinum* were killed at the indicated time periods, and the median number of tissues containing granulomas was determined. Each individual fish is represented as a single point, and the medians are shown as overlying bar graphs (white for the 5-CFU group and dark gray for the 60-CFU group). Multiple fish at a given time point having the same number of tissues involved are shown as a white numeral within the symbols (■ or ●). Tissues examined included liver, kidney, pancreas, gonads, and mesentery. The significance in the differences in the extent of granulomatous disease between the two doses was determined using the Mann-Whitney test (**, $P < 0.05$).

duced feeding and weakened swimming for approximately 1 week. The fish either were often listless at the bottom of the tank or exhibited listless piping, remaining at the surface, constantly opening and closing their mouths in an attempt to increase gas exchange (32). Dying fish also frequently had external red lesions on the trunk ventral to the lateral line and in close proximity to internal organs, ascites, and exophthalmia, the latter two signs being indicators of kidney failure and osmoregulatory stress (47).

Disease progression was assessed in the second cohort of infected fish by serial bacterial counts (Fig. 1B to D) and histopathology at 1, 8, and 11 days for the highest dose and 1, 2, 4, 8, and 16 weeks postinfection for the two lower doses. The small size of the zebrafish allowed a determination of total bacterial counts in the whole animal without separating organs (40). For all doses, bacterial counts increased to reach a plateau of 6 to 7 logs at times postinfection that correlated inversely with the infecting dose (Fig. 1B and C). A few of the survivors had overt signs of disease, while the others appeared healthy. Of the fish that survived to the 16-week time point, two in the group infected with 5 CFU had counts that were below 3.4 logs, the level of detection in these experiments, while two other fish (one from each group) had counts that were markedly lower than those of the other fish

(Fig. 1B). Because these fish were sampled from the surviving population, which was likely enriched for fish that may have been misinjected, it was probable that these fish were never infected with *M. marinum*. This notion was further supported by the finding that three of the surviving fish in the 5-CFU group showed no evidence of active or healing infection by histology, while the remainder of the fish in both groups showed extensive granulomatous disease (data not shown). The two fish with very low bacterial counts may have been initially uninfected and may have become infected later from dying fish in the same tank, although we cannot rule out the possibility that they were in the process of clearing the infection. The median bacterial counts between 4, 8, and 16 weeks of infection in the 60-CFU group and 8 and 16 weeks in the 5-CFU group were not significantly different by analysis of variance (ANOVA). Similarly, the bacterial burden in the 8,970-CFU group did not change significantly between 8 and 11 days and was not significantly different from the final counts achieved in the 5- and 60-CFU groups, as determined by ANOVA, confirming that the bacterial counts plateau to a fixed level, regardless of the initial dose.

The extent of *M. marinum* granulomatous disease is time- and dose-dependent. The small size of the zebrafish permitted a histological assessment of the progression and dissemination of the infection in the entire fish by examining sagittal sections in which the organs were well represented. Serial sections could be used for different histological stains of the same granulomas. In the 5- and 60-CFU groups, the extent of granulomatous pathology increased over time and correlated with progressive mortality and an increase in bacterial burden (Fig. 1A, C, and D). At 1 week, granulomas were evident in only one fish in each group, whereas at later time points, granulomas were readily detected in most fish. Granulomas were frequently found in the mesentery, pancreas, gonads, kidney, and liver but rarely in the head, branchial arches, and spleen and never in the muscle or skin.

The extent of disease was scored by assessing the number of regions and/or organs involved by granulomatous disease in each fish. The number of regions involved increased with time for the 60-CFU dose (Fig. 1D). By week 4, there was a significant difference in the extent of disease between the 5- and 60-CFU doses, mirroring the differences in bacterial CFU and host survival between these doses at this time point (Fig. 1B). Owing to mortalities by the 8-week time point, only two fish were available for histological analysis in the 5-CFU group, and none were available in the 60-CFU group. These two fish both had five regions involved, similar to the extent of disease seen in the 60-CFU group at 4 weeks. This increase in disease burden in the fish that received the lower dose again mirrors the pattern in the bacterial counts, with increasing bacterial burden correlating with disease dissemination (Fig. 1B and D). Consistent with the accelerated mortality and bacterial counts seen in the fish infected with 8,970 CFU, this inoculum produced extensive disease involving most regions by 8 days postinfection (data not shown).

Progression of granuloma pathology is also both time- and dose-dependent. A detailed analysis of progression of granuloma pathology was performed for the fish infected with 5 CFU. For the first 2 weeks after infection, nonnecrotizing lesions were predominant, and early macrophage aggregates with cytoplasmic and nuclear debris, likely representing early necrosis, were seen (Fig. 2A and B). By 16 weeks, approximately equal numbers of well-organized but nonnecrotizing and necrotizing granulomas were present (Fig. 2C to F). The clear areas in Fig. 2C likely reflect either the beginnings of cellular breakdown to form necrotic zones or less interdigitation of the cells. An example of an early necrotic focus is shown in Fig. 2E and F, where cellular remnants are seen in the partially necrotic area but not in the completely necrotic area. The bacteria were found predominantly in necrotic areas and were in greater numbers in fully necrotic than in partially necrotic zones (Fig. 2F). As a result, necrotizing lesions had far greater numbers of bacteria than did nonnecrotizing granulomas (Fig. 2, compare B and D to F and H). At 16 weeks, necrotic lesions predominated, and thin-walled lesions with prominent necrosis were found (Fig. 2G and H), as has been previously reported for human granulomas in the setting of active disease (53). Also prominent at this time point were multicentric granulomas (Fig. 2I and J), which again were similar to lesions found in late-stage human tuberculosis (53). Progression to necrotizing infection was also dose dependent, appearing by day 8 in the 60- and 8,970-CFU groups and being predominant at the highest dose at both days 8 and 11 (see Fig. S1 in the supplemental material).

Despite extensive examination of numerous fish at all doses and time points, we found no lesions similar to those seen during chronic asymptomatic tuberculous infection of humans as determined by Von Kossa staining for the presence of calcification and trichrome staining for the presence of fibrosis (data not shown). A feature specific to fish and frogs was the accumulation of pigment in the later stages of disease (Fig. 2I and J). This pigment is likely associated with melanomacrophages. Melanomacrophages are capable of phagocytosing and eliminating bacterial pathogens in other fish diseases (6), but their potential role in mycobacterial disease pathogenesis remains unexplored (5, 33, 48).

Similar to frog and goldfish lesions, zebrafish *M. marinum* granulomas contained few lymphocytes as judged by hematoxylin and eosin staining (compare Fig. 2A, C, and E). This feature is in contrast to *M. tuberculosis* granulomas in mice, humans, and nonhuman primates and *M. marinum* granulomas in humans (14). The abundance of lymphocytes does not appear to be related to the presence of necrosis, as zebrafish, goldfish, and frog *M. marinum* granulomas all show few lymphocytes, yet the former two hosts readily form necrotizing lesions.

Zebrafish lacking *rag1* are hypersusceptible to *M. marinum* infection. Cell-mediated adaptive immunity plays a critical protective role in mammalian tuberculosis (21), and the paucity of lymphocytes in zebrafish granulomas suggested that the role of the adaptive immune response to mycobacteria might be less important in this host. The recent availability of a targeted *rag1* knockout fish (58) allowed us to test the role of lymphocytes in protection against mycobacterial infection in the fish. Fish lacking *rag1* do not undergo VDJ recombination and thus lack functional T and B cells (58). We infected isogenic $rag1^{-/-}$, $rag1^{+/-}$, and $rag1^{+/+}$ zebrafish siblings with *M. marinum* and compared their survival rates and disease pathologies. The genotype of each fish was confirmed prior to infection, and the

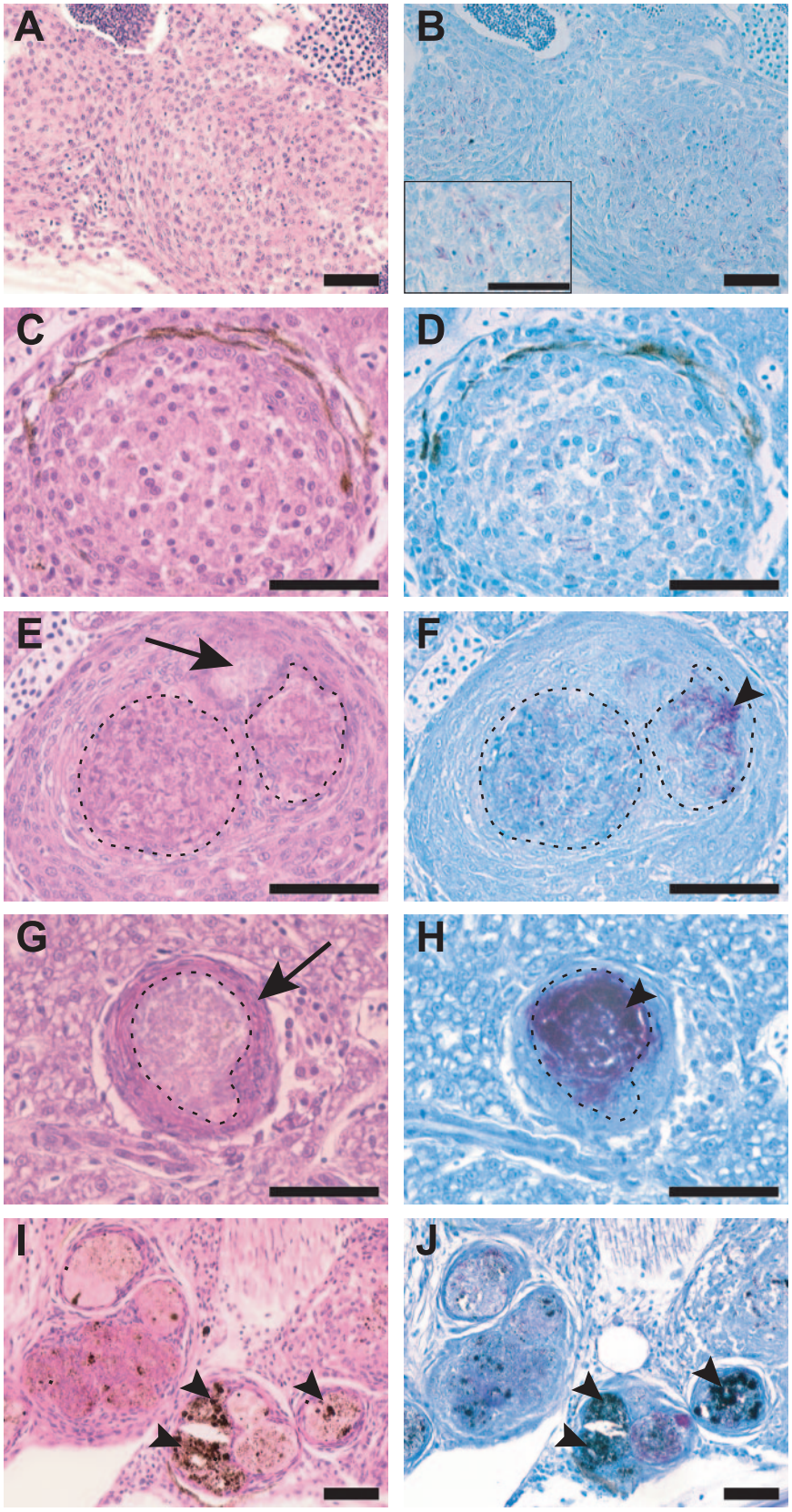

FIG. 2. Zebrafish tuberculosis disease progression is characterized by progressive necrosis and pigment deposition with large numbers of bacteria found within necrotic granulomas. Adult zebrafish were infected with 5 CFU of wild-type *M. marinum*, and histology was assessed at 2 weeks (A and B), 8 weeks (C, D, E, and F), and 16 weeks (G, H, I, and J) postinfection with hematoxylin and eosin (A, C, E, G, and I) and

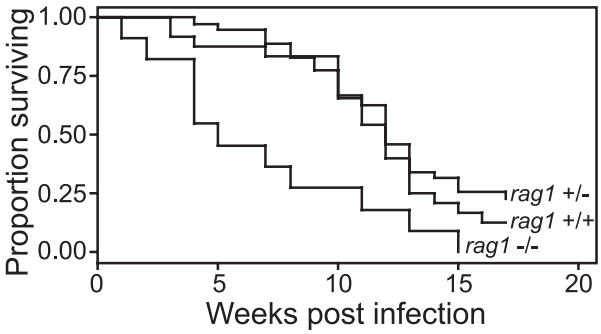

FIG. 3. Zebrafish lacking *rag1* are hypersusceptible to infection by *M. marinum*. Twelve *rag1* wild-type, heterozygous, or mutant fish were infected with 8 CFU of WT bacteria and reared in separate tanks. Each tank was monitored for mortalities over a 16-week period. A Kaplan-Meier curve was calculated for each group of fish, and compared to *rag1* WT or heterozygous fish, *rag1* mutant animals showed a significant difference in survival as calculated by log-rank test ($P = 0.002$). The Cox proportional hazards model was used to quantify the differences between groups and confirmed significant differences in survival between mutant and wild-type fish (HR = 2.7; 95% CI = 1.6 to 4.7; $P < 0.0001$) and mutant and heterozygous fish (HR = 3.2; 95% CI = 2.1 to 4.8; $P < 0.0001$). There was no significant difference in survival between WT and heterozygous fish (HR = 0.86; 95% CI = 0.46 to 1.63; $P = 0.654$).

rag1 mutant fish raised in our facility appeared healthy but did not spawn as well as their wild-type or heterozygote siblings.

In four experiments using fish spawned at different times and a range of *M. marinum* infection doses (8 to 54 CFU), $rag1^{-/-}$ fish showed significantly increased mortality compared to their $rag1^{+/-}$ and $rag1^{+/+}$ siblings (Fig. 3). Fish that died had extensive granulomatous disease that was the likely the cause of their death. This observation shows that, similar to mammalian hosts infected with *M. tuberculosis*, adaptive immunity plays a critical role in protection against pathogenic mycobacteria in the fish.

A small cohort of isogenic $rag1^{-/-}$, $rag1^{+/-}$, and $rag1^{+/+}$ zebrafish siblings was infected with 25 CFU of *M. marinum* to compare the pathologies at early time points. Infected fish were examined at 6 weeks, and all showed evidence of granuloma formation. Similar to heterozygous and wild-type fish, *rag1* mutant fish formed both nonnecrotizing and necrotizing lesions (data not shown). While the number of fish available for this assessment was too small to make quantitative comparisons of the histopathology of *rag1* mutant and wild-type fish, these preliminary data suggest that granuloma formation and necrosis are independent of adaptive immunity.

***M. marinum* ΔRD1 attenuation in adult zebrafish is associated with defects in granuloma formation.** To further validate our model, we next sought to determine if bacterial mutants that are attenuated in other model systems are similarly attenuated in adult zebrafish. *M. tuberculosis* strains with mutations in the RD1 region are attenuated for growth and virulence in a mouse infection model (26, 28, 45), and RD1-deficient *M. marinum* strains are attenuated in frogs and zebrafish (22, 56). In the zebrafish embryo infection model, macrophages infected with ΔRD1 show an impaired ability to aggregate (56). We wished to determine if this impaired macrophage aggregation correlated with the attenuation of the ΔRD1 mutant when infection was initiated in the context of adaptive immunity. We also wished to address the possibility that macrophage lineages could be distinct in adult and embryonic fish so that the defects observed in the embryo might be specific to bacterial interactions with embryonic macrophages.

Fish were infected with 1,318 CFU of *M. marinum* ΔRD1 or 50 CFU of wild-type *M. marinum*, and host survival was monitored over a 16-week period. Similar to previous findings (22), ΔRD1 caused significantly delayed mortality despite its 26-fold-higher infection dose (Fig. 4A), underscoring the severe attenuation of the ΔRD1 strain previously reported in a variety of animal models. The bacterial burden of the ΔRD1-infected survivors at 16 weeks reached a median of 5.71 logs (range, 5.32 to 7.23 logs) and, by ANOVA, was found to be not significantly different from the plateau of bacterial counts attained for all three doses of wild-type infection described above (Fig. 1B and C). This result is in contrast to a previous report that showed lower bacterial counts in fish infected with RD1 mutant bacteria than in fish infected with wild-type bacteria at early time points (22) but is in agreement with the observation that mice infected with ΔRD1 *M. tuberculosis* eventually reach high bacterial burdens if observed long enough, with some resultant host mortality (45).

ΔRD1 infection of 1-day-old zebrafish embryos results in delayed macrophage aggregation, and this macrophage aggregation defect persists in fish reared to 1 month of age as evidenced by loose, poorly formed, nonnecrotic aggregates (56). To determine if the attenuation phenotype of the ΔRD1 strain seen in adult fish was also associated with these histological differences, individual wild-type and ΔRD1 granulomas were scored in a blinded fashion for the presence of necrosis, whether they were solitary granulomas or in multicentric aggregates, and, in the case of nonnecrotizing granulomas, whether the cellular association was loose or compact (Fig. 4B, C, and D). Because the cohort of fish infected with wild-type bacteria at the same time as the ΔRD1 strain did not survive to be included in this analysis, we instead compared the ΔRD1 lesions to lesions from the 16-week survivors of the wild-type-infected fish described above. Although the two groups of fish

Ziehl-Neelson (B, D, F, H, and J) staining of serial sections. (A and B) Early, loosely associated, nonnecrotic lesions (arrows) with early cellular breakdown in the gonad (teste) composed of an epithelioid macrophage infiltrate surrounding scattered mycobacteria. The inset in B shows a higher-magnification view of acid-fast bacteria residing within macrophages. (C and D) Well-organized, nonnecrotizing granuloma in the liver with clear areas between macrophages reflecting either early necrosis or less interdigitation of the macrophages. (E and F) Necrotizing granuloma in the liver with areas of partial (dashed lines) and complete (arrow) necrosis and acid-fast bacilli (arrowheads) residing predominantly within the necrotic areas. (G and H) Late-stage lesion in the liver with a thin, well-defined macrophage border (arrow) and prominent central necrosis (dashed lines). Note the high bacterial numbers present in the central, necrotic core in H (arrowhead). (I and J) Multicentric necrotic lesions in the head kidney during late-stage disease with extensive pigment deposition (arrowheads). Scale bars, 50 μm. Magnifications, ×200 for A, B, I, and J and ×400 for all other panels.

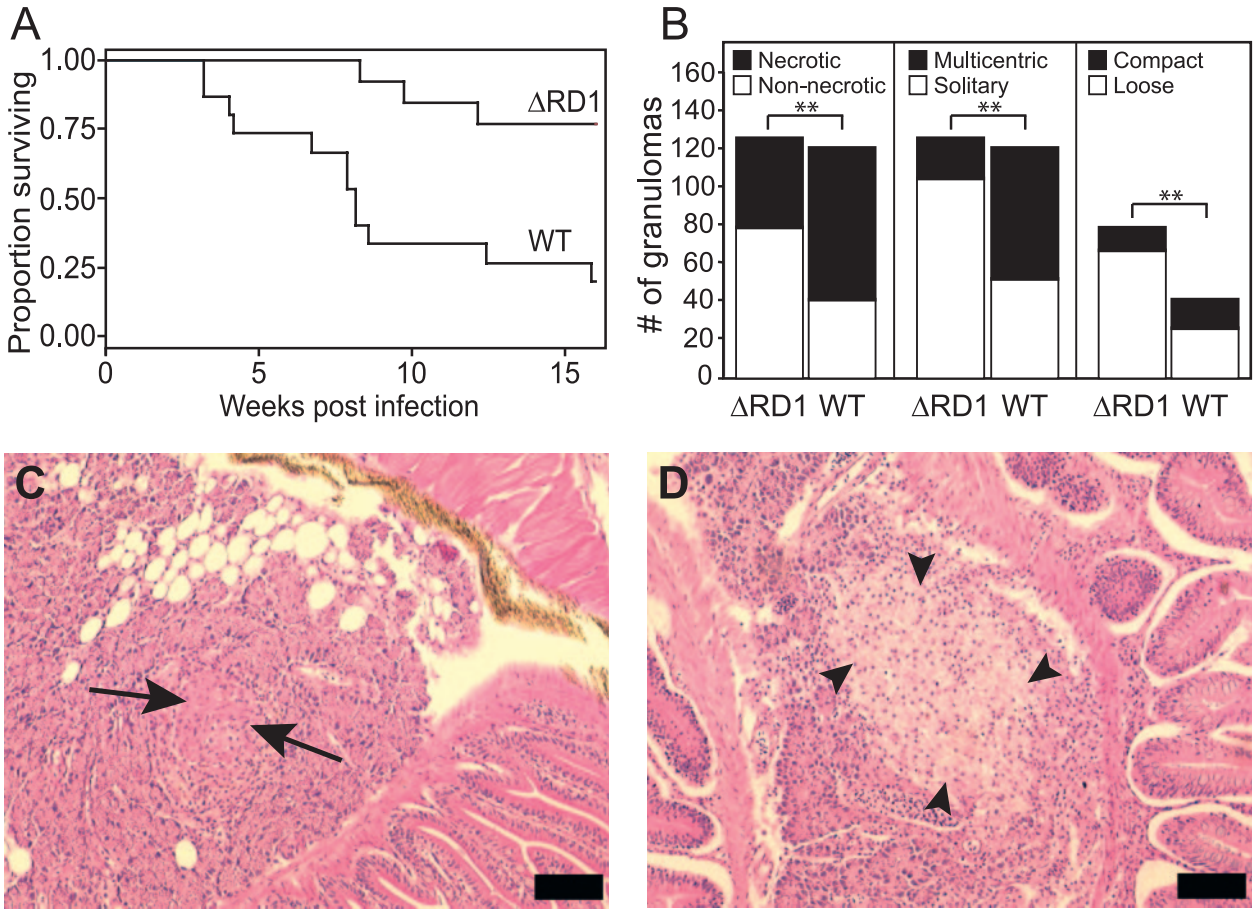

FIG. 4. ΔRD1 is attenuated in adult zebrafish and produces a greater proportion of solitary, loosely associated, nonnecrotic granulomas than does infection with WT *M. marinum*. (A) Survival of adult zebrafish infected with WT or ΔRD1. Fifteen fish were injected with 50 CFU of WT or 1,318 CFU of ΔRD1 bacteria and were reared in separate tanks. Each tank was monitored for mortalities over a 16-week time period. A Kaplan-Meier curve was calculated for each group of fish, and compared to WT-infected fish, ΔRD1-infected fish showed a significant difference in survival as calculated by the log-rank test ($P = 0.0012$). The Cox proportional hazards model was used to quantify the difference between WT- and ΔRD1-infected fish and confirmed significantly increased survival in the ΔRD1-infected fish, with an HR of 0.1592, a 95% CI of 0.04 to 0.57, and a P value of 0.005. (B) ΔRD1 granulomas are more likely to be solitary, nonnecrotizing, and loosely associated than are WT lesions. A total of 121 WT and 126 ΔRD1 granulomas in infected fish at 16 weeks were scored in a blinded fashion for the presence of necrosis and residence in a multicentric lesion. The subset of nonnecrotic lesions was further assessed for the nature of cellular association (compact or loose). Differences in the proportion of granulomas falling into each group were assessed using contingency tables to calculate RR and 95% CI, assigning ΔRD1 as the experimental group and the wild type as the control group. Significance was determined using Fisher's exact test (**, $P < 0.05$). Values obtained for nonnecrotic lesions were an RR of 1.850, a 95% CI of 1.394 to 2.456, and a P value of <0.0001; values obtained for solitary lesions were an RR of 1.939, a 95% CI of 1.557 to 2.415, and a P value of <0.0001; values obtained for loose lesions were an RR of 1.337, a 95% CI of 1.041 to 1.718, and a P value of 0.0111. (C and D) Histopathology of adult zebrafish infected for 16 weeks with either 100 CFU of WT (C) or 1,318 CFU of ΔRD1 (D) bacteria. Median bacterial loads at the time of examination were not significantly different ($P = 0.17$ by Mann-Whitney test). Hematoxylin and eosin staining of pancreatic lesions is shown. Arrows indicate compact, tightly interdigitated epithelioid macrophages in C, while arrowheads in D show loosely associated macrophage aggregates with minimal epithelioid transformation. Scale bars, 50 μm. Magnification, ×100.

were from different initial cohorts, they were bred from the same original AB stocks and were analyzed at the same time point after infection (16 weeks), at which time all fish also had similar median bacterial burdens. This analysis showed that the proportions of nonnecrotizing and solitary granulomas were significantly higher in ΔRD1-infected fish than in fish infected with wild-type bacteria (Fig. 4B). In addition, the proportion of loosely aggregated nonnecrotic lesions was also significantly higher in ΔRD1-infected fish (Fig. 4B and D). These observations suggest that the RD1 locus influences the formation of tight macrophage aggregates during both embryonic and adult infection and plays a role in granuloma necrosis during adult infection.

DISCUSSION

The construction of a flowthrough zebrafish facility has allowed us to conduct detailed longitudinal studies of the course and pathology of *M. marinum* infection in large numbers of adult zebrafish. Our study of *M. marinum*-induced tuberculosis in the zebrafish highlights features shared with active human tuberculosis (53). The hallmark lesion of active tuberculosis,

necrotizing granulomas with abundant bacteria in the necrotic areas (14, 15, 53), is the predominant lesion at late stages of zebrafish disease. We took advantage of the first targeted zebrafish mutant, deficient in *rag1*, to demonstrate that lymphocytes play the same critical role in controlling tuberculosis in zebrafish and mammals and extended the finding that bacterial mutants lacking the RD1 locus are attenuated in adult fish by showing that this attenuation is associated with the formation of loose macrophage aggregates and a paucity of necrotic lesions.

Adult zebrafish are exquisitely sensitive to infection with *M. marinum* strain M; inoculation of 5 CFU virtually always results in chronic granulomatous disease. The mortality rate, early bacterial burdens, and progression of granulomatous pathology are dose dependent, making the zebrafish an ideal animal model to test the virulence of bacterial mutants. Different *M. marinum* strains exhibit different virulences in this model system (54). Human-derived isolates tend to be more virulent for fish and form a distinct genetic cluster, suggesting a genetic basis for this increased virulence. Our work lends further support to this notion, as similar studies using a fish-adapted strain (ATCC 927) required much higher doses of bacteria to achieve similar disease states (40).

By using a range of inocula, we found that ~9,000 bacteria produce acute, fulminant disease. The fish died within 10 days, with extensive disease and high bacterial burdens. These data extend previous reports where much higher doses of *M. marinum* M caused rapid death (22, 23). In contrast, we and others found that lower inocula produce chronic disease (40), similar to the chronic wasting mycobacterioses of aquarium fish recognized by tropical fish culturists. The dose required to cause disease during natural infection is unknown, but it is likely to come from water contaminated by infected fish or from biofilms in the environment or system equipment, making it likely to be low. The 5-CFU dose may simulate a natural disease course, producing a chronic, long-term infection despite ultimately achieving bacterial burdens and extent of granulomatous disease similar to those of fish infected with higher doses. A similar relationship between bacterial dose and disease outcome has previously been described for goldfish and medaka infected with *M. marinum* (7, 48). It is likely that high doses overwhelm the immune system rapidly, whereas the low doses allow the generation of partially protective innate and adaptive immune responses.

The presence of necrosis in the zebrafish granulomas distinguishes them from *M. marinum* granulomas in the leopard frog as well as *M. tuberculosis* granulomas in the commonly used mouse model of infection (5, 20, 53). In this regard, they are similar to *M. marinum* infection of other fish species (7, 24, 48) and humans (3) and to *M. tuberculosis* infection of humans, nonhuman primates, rabbits, and guinea pigs (2, 8, 15, 16, 29, 53). Therefore, the presence of necrosis in tuberculous granulomas appears to be at least partially determined by host factors. The progression of necrosis to thin-walled cavities full of necrotic material mirrors that found in human tuberculosis (53). In contrast, leopard frogs are also highly susceptible to *M. marinum* infection (~10 CFU establishes infection), but even doses as high as 7 logs lead to long-term asymptomatic infection rather than active disease (41). Infected frogs also do not develop necrotic granulomas even with high inocula. It is possible that the absence of necrosis indicates an increased resistance to infection, although many other species-specific differences in immunity likely exist. There is considerable debate and uncertainty about the role and nature of necrosis, the physiological and replicative state of the bacteria residing within necrotic lesions, and their potential contribution to the antibiotic tolerance that makes tuberculosis so difficult to treat (14, 25). Little is known about the host and bacterial factors that contribute to the formation of caseous necrosis, and the genetic tractability of both the zebrafish and *M. marinum* should help to address this question. Indeed, our results show that the RD1 locus influences the formation of necrosis.

In contrast to human and some nonhuman models, zebrafish do not appear to clear pathogenic mycobacterial infection, even at low infecting doses. No significant evidence of healing, such as fibrosis or calcification, was seen in the many infected animals that we examined (data not shown). Combined with previous studies of *M. marinum* pathogenesis in fish and frogs (22, 40, 41, 48, 54), our results suggest that the zebrafish is a good model system for the study of active, caseating tuberculosis rather than latent disease, while the frog provides a good model for indefinitely asymptomatic infection mimicking latent human disease.

Unlike mammalian tuberculous granulomas, zebrafish lesions have very few lymphocytes. In this way, they are similar to frog and goldfish granulomas (5, 48) and distinct from *M. marinum*-induced human granulomas (3). Based on these observations, the number of lymphocytes in tuberculous granulomas is likely to be host mediated rather than due to differences between *M. marinum* and *M. tuberculosis* in promoting lymphocyte infiltration of granulomas. Zebrafish have T lymphocytes that populate and exit the thymus in ways similar to those of mammals (27, 52). Indeed, in silico analysis of the zebrafish genome suggests that zebrafish share the same T-lymphocyte subsets as mammals (52). Fluorescence-activated cell sorter analysis of zebrafish peripheral blood showed that lymphocytes are present, albeit at reduced ratios compared to those seen in mice and humans (51).

Given the paucity of lymphocytes in granulomas, it was important to determine if they played a functional role in the control of zebrafish tuberculosis. *rag1* mutant fish die more rapidly from *M. marinum* infection, similar to *rag1* mutant mice infected with *M. tuberculosis* (44). These *rag1* mutant fish do form granulomas, even necrotic ones. Thus, we conclude that adaptive immunity does play an important role in the protection against mycobacterial disease in the fish, suggesting that the few lymphocytes in zebrafish granulomas are functionally equivalent to the many lymphocytes found in mammals. These data corroborate our studies of zebrafish embryos showing that granuloma formation occurs as a result of bacterial interactions with innate immunity (18). Similar to *M. tuberculosis* growth kinetics in mice, rabbits, or guinea pigs (17, 34), *M. marinum* grows exponentially over the first few weeks after infection, followed by a leveling of bacterial numbers. This plateau in bacterial burden correlates with the onset of the adaptive immune response in mammalian hosts (17, 34), suggesting that the onset of the adaptive immunity in fish is similarly responsible for curtailing bacterial growth. Indeed, the likely reason for the higher mortality observed in the *rag1* mutant fish is a failure to control bacterial growth, despite

grossly normal granuloma formation. More detailed studies will be required to determine the impact of adaptive immunity on the kinetics of bacterial growth as well as granuloma formation and the maintenance of granuloma structure.

Finally, we confirm the finding that *M. marinum* strains lacking the RD1 locus are attenuated in adult zebrafish (22) as they are in embryos and adult frogs (56). A previous report using much higher infection doses (10^3 to 10^5 CFU), shorter observation periods, and different RD1 mutants than the one used in our study showed lower bacterial counts and longer survival in zebrafish infected with the mutant bacteria (22). Our extended analysis reveals that, at least for the mutant used in our studies, bacteria lacking RD1 ultimately reach a similar plateau as wild-type bacteria and that this increased bacterial burden is associated with some host mortality. These results are similar to those obtained for *M. tuberculosis* ΔRD1 infection of mice, where high organism burdens are ultimately reached with some resultant host mortality (45), and have important implications for the use of strains lacking the RD1 region as vaccine candidates (45). Low-dose (5- to 50-CFU) infections with the various RD1 mutant bacteria will help to clarify whether the differences in doses, observation times, and/or the actual nature of the RD1 mutants account for the different outcomes observed in the two zebrafish studies.

In previous studies, we have taken advantage of the optical transparency of zebrafish embryos to determine the steps at which bacterial virulence determinants impact infection (13, 56). Infection of embryos with the ΔRD1 mutant results in delayed macrophage aggregation, suggesting that this locus promotes granuloma formation. ΔRD1-infected adult fish form a greater proportion of nonnecrotizing, solitary, and loose aggregates than do fish infected with wild-type *M. marinum*, suggesting that macrophage aggregation is impaired even in the context of adult-lineage macrophages and adaptive immunity. Based on our embryo work, we had proposed that the lack of RD1 resulted in delayed kinetics of granuloma formation (56). In the adult fish, we saw predominantly solitary, loose aggregates with a few well-formed and even necrotic granulomas. These findings also suggest a kinetic defect in granuloma formation rather than an absolute defect that is associated with an attenuation in bacterial virulence. These kinetic differences appear to have a significant impact on virulence, as even much higher inocula of the ΔRD1 mutant take much longer to plateau to wild-type levels and cause limited death of the infected host. Taken together, these observations suggest that mycobacterial virulence factors such as RD1 contribute to pathogenesis by altering the kinetics of the host response throughout the course of infection.

In conclusion, this study extends the findings of others and lays the groundwork for the use of the adult zebrafish to study a variety of aspects of tuberculosis ranging from immunology to pathogenesis and drug tolerance in a facile, small animal model of active necrotizing disease.

ACKNOWLEDGMENTS

We thank Lance Squires and Josh Brown of Aquatic Habitats for their assistance with designing the flowthrough system, Artemis Pharmaceuticals for providing the *rag1* zebrafish strain, Allan Decamp for help with statistical analysis of the survival assays, José de la Torre for assistance in assembling figures and discussions regarding statistical analysis, Mark Troll and Christine Cosma for advice regarding statistical analysis, Robin Lesley for help with figure design and technical assistance, and members of the Ramakrishnan laboratory for discussions.

L.E.S. dedicates this paper to the memory of Marsha Landolt, former director of the School of Aquatic and Fisheries Sciences and Dean of the Graduate School of the University of Washington.

This work was supported by National Institutes of Health grants RO1 AI036396 and RO1 AI54503 and a Burroughs Wellcome award to L.R. L.E.C. was supported by a Pfizer Pharmaceuticals postdoctoral fellowship in infectious diseases, and H.E.V. was supported by an American Heart Association predoctoral fellowship.

REFERENCES

1. **Adams, D. O.** 1976. The granulomatous inflammatory response. A review. Am. J. Pathol. **84:**164–191.
2. **Balasubramanian, V., E. H. Wiegeshaus, and D. W. Smith.** 1994. Mycobacterial infection in guinea pigs. Immunobiology **191:**395–401.
3. **Bartralot, R., R. M. Pujol, V. Garcia-Patos, D. Sitjas, N. Martin-Casabona, P. Coll, A. Alomar, and A. Castells.** 2000. Cutaneous infections due to nontuberculous mycobacteria: histopathological review of 28 cases. Comparative study between lesions observed in immunosuppressed patients and normal hosts. J. Cutan. Pathol. **27:**124–129.
4. **Barut, B. A., and L. I. Zon.** 2000. Realizing the potential of zebrafish as a model for human disease. Physiol. Genomics **2:**49–51.
5. **Bouley, D. M., N. Ghori, K. L. Mercer, S. Falkow, and L. Ramakrishnan.** 2001. Dynamic nature of host-pathogen interactions in *Mycobacterium marinum* granulomas. Infect. Immun. **69:**7820–7831.
6. **Brattgjerd, S., and O. Evensen.** 1996. A sequential light microscopic and ultrastructural study on the uptake and handling of *Vibrio salmonicida* in phagocytes of the head kidney in experimentally infected Atlantic salmon (*Salmo salar L.*). Vet. Pathol. **33:**55–65.
7. **Broussard, G. W., and D. G. Ennis.** 2006. *Mycobacterium marinum* produces long-term chronic infections in medaka: a new animal model for studying human tuberculosis. Comp. Biochem. Physiol., in press.
8. **Capuano, S. V., III, D. A. Croix, S. Pawar, A. Zinovik, A. Myers, P. L. Lin, S. Bissel, C. Fuhrman, E. Klein, and J. L. Flynn.** 2003. Experimental *Mycobacterium tuberculosis* infection of cynomolgus macaques closely resembles the various manifestations of human *M. tuberculosis* infection. Infect. Immun. **71:**5831–5844.
9. **Casanova, J. L., and L. Abel.** 2002. Genetic dissection of immunity to mycobacteria: the human model. Annu. Rev. Immunol. **20:**581–620.
10. **Clark, H. F., and C. C. Shepard.** 1963. Effect of environmental temperatures on infection with *Mycobacterium marinum* (Balnei) of mice and a number of poikilothermic species. J. Bacteriol. **86:**1057–1069.
11. **Cosma, C. L., J. M. Davis, L. E. Swaim, H. Volkman, and L. Ramakrishnan.** Zebrafish and frog models of *Mycobacterium marinum* infection. *In* Current Protocols in Microbiology, in press.
12. **Cosma, C. L., O. Humbert, and L. Ramakrishnan.** 2004. Superinfecting mycobacteria home to established tuberculous granulomas. Nat. Immunol. **5:**828–835.
13. **Cosma, C. L., K. Klein, R. Kim, D. Beery, and L. Ramakrishnan.** 2006. *Mycobacterium marinum* Erp is a virulence determinant required for cell wall integrity and intracellular survival. Infect. Immun. **74:**3125–3133.
14. **Cosma, C. L., D. R. Sherman, and L. Ramakrishnan.** 2003. The secret lives of the pathogenic mycobacteria. Annu. Rev. Microbiol. **57:**641–676.
15. **Dannenberg, A. M., Jr.** 1993. Immunopathogenesis of pulmonary tuberculosis. Hosp. Pract. **28:**51–58.
16. **Dannenberg, A. M., Jr.** 2001. Pathogenesis of pulmonary *Mycobacterium bovis* infection: basic principles established by the rabbit model. Tuberculosis (Edinburgh) **81:**87–96.
17. **Dannenberg, A. M., Jr., and F. M. Collins.** 2001. Progressive pulmonary tuberculosis is not due to increasing numbers of viable bacilli in rabbits, mice and guinea pigs, but is due to a continuous host response to mycobacterial products. Tuberculosis (Edinburgh) **81:**229–242.
18. **Davis, J. M., H. Clay, J. L. Lewis, N. Ghori, P. Herbomel, and L. Ramakrishnan.** 2002. Real-time visualization of Mycobacterium-macrophage interactions leading to initiation of granuloma formation in zebrafish embryos. Immunity **17:**693–702.
19. **Decostere, A., K. Hermans, and F. Haesebrouck.** 2004. Piscine mycobacteriosis: a literature review covering the agent and the disease it causes in fish and humans. Vet. Microbiol. **99:**159–166.
20. **Flynn, J. L.** 2006. Lessons from experimental *Mycobacterium tuberculosis* infections. Microbes Infect. **8:**1179–1188.
21. **Flynn, J. L., and J. Chan.** 2001. Immunology of tuberculosis. Annu. Rev. Immunol. **19:**93–129.
22. **Gao, L. Y., S. Guo, B. McLaughlin, H. Morisaki, J. N. Engel, and E. J. Brown.** 2004. A mycobacterial virulence gene cluster extending RD1 is required for cytolysis, bacterial spreading and ESAT-6 secretion. Mol. Microbiol. **53:**1677–1693.
23. **Gao, L. Y., M. Pak, R. Kish, K. Kajihara, and E. J. Brown.** 2006. A myco-

bacterial operon essential for virulence in vivo and invasion and intracellular persistence in macrophages. Infect. Immun. **74:**1757–1767.
24. **Gauthier, D. T., M. W. Rhodes, W. K. Vogelbein, H. Kator, and C. A. Ottinger.** 2003. Experimental mycobacteriosis in striped bass *Morone saxatilis*. Dis. Aquat. Organ. **54:**105–117.
25. **Grosset, J.** 2003. *Mycobacterium tuberculosis* in the extracellular compartment: an underestimated adversary. Antimicrob. Agents Chemother. **47:** 833–836.
26. **Guinn, K. M., M. J. Hickey, S. K. Mathur, K. L. Zakel, J. E. Grotzke, D. M. Lewinsohn, S. Smith, and D. R. Sherman.** 2004. Individual RD1-region genes are required for export of ESAT-6/CFP-10 and for virulence of *Mycobacterium tuberculosis*. Mol. Microbiol. **51:**359–370.
27. **Langenau, D. M., A. A. Ferrando, D. Traver, J. L. Kutok, J. P. Hezel, J. P. Kanki, L. I. Zon, A. T. Look, and N. S. Trede.** 2004. In vivo tracking of T cell development, ablation, and engraftment in transgenic zebrafish. Proc. Natl. Acad. Sci. USA **101:**7369–7374.
28. **Lewis, K. N., R. Liao, K. M. Guinn, M. J. Hickey, S. Smith, M. A. Behr, and D. R. Sherman.** 2003. Deletion of RD1 from *Mycobacterium tuberculosis* mimics bacille Calmette-Guerin attenuation. J. Infect. Dis. **187:**117–123.
29. **McMurray, D. N.** 2003. Hematogenous reseeding of the lung in low-dose, aerosol-infected guinea pigs: unique features of the host-pathogen interface in secondary tubercles. Tuberculosis (Edinburgh) **83:**131–134.
30. **Meijer, A. H., F. J. Verbeek, E. Salas-Vidal, M. Corredor-Adamez, J. Bussman, A. M. van der Sar, G. W. Otto, R. Geisler, and H. P. Spaink.** 2005. Transcriptome profiling of adult zebrafish at the late stage of chronic tuberculosis due to *Mycobacterium marinum* infection. Mol. Immunol. **42:**1185–1203.
31. **Nasevicius, A., and S. C. Ekker.** 2000. Effective targeted gene 'knockdown' in zebrafish. Nat. Genet. **26:**216–220.
32. **Noga, E. J.** 1996. Fish disease: diagnosis and treatment. Mosby-Year Book, St. Louis, Mo.
33. **Noga, E. J., J. F. Wright, and L. Pasarell.** 1990. Some unusual features of mycobacteriosis in the cichlid fish *Oreochromis mossambicus*. J. Comp. Pathol. **102:**335–344.
34. **North, R. J., and Y. J. Jung.** 2004. Immunity to tuberculosis. Annu. Rev. Immunol. **22:**599–623.
35. **Opie, E. L., and J. D. Aronson.** 1927. Tubercle bacilli in latent tuberculous lesions and in lung tissue without tuberculous lesions. Arch. Pathol. Lab. Med. **4:**1–21.
36. **Patton, E. E., and L. I. Zon.** 2001. The art and design of genetic screens: zebrafish. Nat. Rev. Genet. **2:**956–966.
37. **Peterson, R. T., and M. C. Fishman.** 2004. Discovery and use of small molecules for probing biological processes in zebrafish. Methods Cell Biol. **76:**569–591.
38. **Peterson, R. T., S. Y. Shaw, T. A. Peterson, D. J. Milan, T. P. Zhong, S. L. Schreiber, C. A. MacRae, and M. C. Fishman.** 2004. Chemical suppression of a genetic mutation in a zebrafish model of aortic coarctation. Nat. Biotechnol. **22:**595–599.
39. **Pozos, T. C., and L. Ramakrishnan.** 2004. New models for the study of Mycobacterium-host interactions. Curr. Opin. Immunol. **16:**499–505.
40. **Prouty, M. G., N. E. Correa, L. P. Barker, P. Jagadeeswaran, and K. E. Klose.** 2003. Zebrafish-*Mycobacterium marinum* model for mycobacterial pathogenesis. FEMS Microbiol. Lett. **225:**177–182.
41. **Ramakrishnan, L., R. H. Valdivia, J. H. McKerrow, and S. Falkow.** 1997. *Mycobacterium marinum* causes both long-term subclinical infection and acute disease in the leopard frog (*Rana pipiens*). Infect. Immun. **65:**767–773.
42. **Sanger Institute.** 12 October 2005, revision date. *Mycobacterium marinum* Sequencing Project. [Online.] http://www.sanger.ac.uk/Projects/M_marinum/.
43. **Sanger Institute.** 20 July 2006, revision date. The *Danio rerio* Sequencing Project. [Online.] http://www.sanger.ac.uk/Projects/D_rerio/.
44. **Saunders, B. M., H. Briscoe, and W. J. Britton.** 2004. T cell-derived tumour necrosis factor is essential, but not sufficient, for protection against *Mycobacterium tuberculosis* infection. Clin. Exp. Immunol. **137:**279–287.
45. **Sherman, D. R., K. M. Guinn, M. J. Hickey, S. K. Mathur, K. L. Zakel, and S. Smith.** 2004. *Mycobacterium tuberculosis* ΔRD1 is more virulent than *M. bovis* BCG in long-term murine infection. J. Infect. Dis. **190:**123–126.
46. **Stamm, L. M., and E. J. Brown.** 2004. *Mycobacterium marinum*: the generalization and specialization of a pathogenic mycobacterium. Microbes Infect. **6:**1418–1428.
47. **Stoskopf, M. K.** 1993. Fish medicine. W. B. Saunders Company, Philadelphia, Pa.
48. **Talaat, A. M., R. Reimschuessel, S. S. Wasserman, and M. Trucksis.** 1998. Goldfish, *Carassius auratus*, a novel animal model for the study of *Mycobacterium marinum* pathogenesis. Infect. Immun. **66:**2938–2942.
49. **Tonjum, T., D. B. Welty, E. Jantzen, and P. L. Small.** 1998. Differentiation of *Mycobacterium ulcerans*, *M. marinum*, and *M. haemophilum*: mapping of their relationships to *M. tuberculosis* by fatty acid profile analysis, DNA-DNA hybridization, and 16S rRNA gene sequence analysis. J. Clin. Microbiol. **36:**918–925.
50. **Traver, D., P. Herbomel, E. E. Patton, R. D. Murphey, J. A. Yoder, G. W. Litman, A. Catic, C. T. Amemiya, L. I. Zon, and N. S. Trede.** 2003. The zebrafish as a model organism to study development of the immune system. Adv. Immunol. **81:**253–330.
51. **Traver, D., B. H. Paw, K. D. Poss, W. T. Penberthy, S. Lin, and L. I. Zon.** 2003. Transplantation and in vivo imaging of multilineage engraftment in zebrafish bloodless mutants. Nat. Immunol. **4:**1238–1246.
52. **Trede, N. S., D. M. Langenau, D. Traver, A. T. Look, and L. I. Zon.** 2004. The use of zebrafish to understand immunity. Immunity **20:**367–379.
53. **Ulrichs, T., and S. H. Kaufmann.** 2006. New insights into the function of granulomas in human tuberculosis. J. Pathol. **208:**261–269.
54. **van der Sar, A. M., A. M. Abdallah, M. Sparrius, E. Reinders, C. M. Vandenbroucke-Grauls, and W. Bitter.** 2004. *Mycobacterium marinum* strains can be divided into two distinct types based on genetic diversity and virulence. Infect. Immun. **72:**6306–6312.
55. **van der Sar, A. M., B. J. Appelmelk, C. M. Vandenbroucke-Grauls, and W. Bitter.** 2004. A star with stripes: zebrafish as an infection model. Trends Microbiol. **12:**451–457.
56. **Volkman, H. E., H. Clay, D. Beery, J. C. Chang, D. R. Sherman, and L. Ramakrishnan.** 2004. Tuberculous granuloma formation is enhanced by a mycobacterium virulence determinant. PLoS Biol. **2:**1946–1956.
57. **Westerfield, M.** 2000. The zebrafish book. A guide for the laboratory use of zebrafish (*Danio rerio*). University of Oregon Press, Eugene, Oreg.
58. **Wienholds, E., S. Schulte-Merker, B. Walderich, and R. H. Plasterk.** 2002. Target-selected inactivation of the zebrafish *rag1* gene. Science **297:**99–102.
59. **Wolf, J. C., and S. A. Smith.** 1999. Comparative severity of experimentally induced mycobacteriosis in striped bass *Morone saxatilis* and hybrid tilapia *Oreochromis* spp. Dis. Aquat. Organ. **38:**191–200.

Editor: J. L. Flynn

INFECTION AND IMMUNITY, Mar. 2007, p. 1540 Vol. 75, No. 3
0019-9567/07/$08.00+0 doi:10.1128/IAI.00069-07

AUTHOR'S CORRECTION

Mycobacterium marinum Infection of Adult Zebrafish Causes Caseating Granulomatous Tuberculosis and Is Moderated by Adaptive Immunity

Laura E. Swaim, Lynn E. Connolly, Hannah E. Volkman, Olivier Humbert, Donald E. Born, and Lalita Ramakrishnan

Departments of Microbiology, Medicine, Immunology, and Pathology and Molecular and Cellular Biology Graduate Program, University of Washington, Seattle, Washington 98195

Volume 74, no. 11, p. 6108–6117, 2006. Page 6109, column 2, line 13: "0.1% 3-aminobenzoic acid ethyl ester (tricaine)" should read "0.02% 3-aminobenzoic acid ethyl ester (tricaine; pH 7.0)."

Line 20: "0.5% tricaine" should read "0.05% tricaine (pH 7.0)."